Thin Solid Films 518 (2010) 6951–6961

Contents lists available at ScienceDirect

Thin Solid Films

journal homepage: www.elsevier.com/locate/tsf

Ab initio study of the binding of collagen amino acids to graphene and A-doped (A = H, Ca) graphene

Claudio Cazorla

Department of Chemistry, UCL, London WC1H 0AJ, UK

ARTICLE INFO

Article history:
Received 5 January 2010
Received in revised form 15 June 2010
Accepted 30 June 2010
Available online 8 July 2010

Keywords:
Density functional theory
Graphene
Graphane
Amino acid

ABSTRACT

We present a theoretical study of the binding of collagen amino acids (AA, namely glycine, Gly; proline, Pro; and hydroxyproline, Hyp) to graphene (Gr), Ca-doped graphene and graphane (Gra) using density functional theory calculations and *ab initio* molecular dynamics (AIMD) simulations. It is found that binding of Gly, Pro and Hyp to Gr and Gra is thermodynamically favorable yet dependent on the amino acid orientation and always very weak (adsorption energies E_{ads} range from −90 to −20 meV). AIMD simulations reveal that room-temperature thermal excitations are enough to induce detachment of Gly and Pro from Gr and of all three amino acids from Gra. Interestingly, we show that collagen AA binding to Gr is enhanced dramatically by doping the carbon surface with calcium atoms (corresponding E_{ads} values decrease by practically two orders of magnitude with respect to the non-doped case). This effect is result of electronic charge transfers from the Ca impurity (donor) to Gr (acceptor) and the carboxyl group (COOH) of the amino acid (acceptor). The possibility of using Gr and Gra as nanoframes for sensing of collagen amino acids has also been investigated by performing electronic density of states analysis. It is found that, whether Gr is hardly sensitive, the electronic band gap of Gra can be modulated by attaching different number and species of AAs onto it. The results presented in this work provide fundamental insights on the quantum interactions of collagen protein components with carbon-based nanostructures and can be useful for developments in bio and nanotechnology fields.

1. Introduction

Recent progress on understanding bio-inorganic interfaces and the physico-chemical processes occurring in them has lead to major developments in a number of scientific areas like nanotechnology, biomedicine, food industry and energy storage production. Intimately related to this progress is the discovery of carbon-based nanostructures (CNSs, nanotubes and fullerenes) [1–3] and surfaces (CSs, graphene and graphane) [4–6], and the refinement of related synthesis processes for mass production [7–9]. CNSs and CSs posses extraordinary electronic, structural and mechanical properties [10–12] which have been exploited in the design and realization of chemical and biological sensors, components of integrated circuits and platforms for hydrogen storage, among other uses [13–18]. Intense research has been also directed on how to employ such intriguing properties in biological and biomedical applications. So far, bio-functionalization techniques based on chemical modification have proved carbon nanotubes (CNTs) as efficient drug-delivery devices, molecular transporters and cell nanoinjectors [19–22].

A promising and rapidly evolving multidisciplinary area within biomedicine is regenerative medicine/tissue engineering which seeks to develop functional cells and tissue to treat or partly cure musculoskeletal injuries and organ disfunctions. The development of biomaterials and scaffolds designed to direct the growth, differentiation and organization of cells in harvesting new functional tissue (*in vivo* or *in vitro*) is required for further advancement on this discipline. CNSs and graphene (one-atom thick planar sheet of carbon atoms densely packed in a honeycomb crystal lattice) appear to be propitious materials for this end since they can be assembled to form three-dimensional porous structures [23] (which are well-known to encourage bone cell ingrowth) and are manageable and also relatively cheap to produce. Up to date, functionalized CNTs have been demonstrated to work as excellent scaffolds in production of directed neuronal networks [24,25] and structural reinforcement of cell-growth nanoframes [26]. In view of these remarkable achievements and present progress on the field of biotechnological applications, gathering knowledge on the interactions between biomolecules important for life and CNSs/CSs is unduly desirable.

In this work, we present a theoretical study of the binding of glycine (Gly), proline (Pro) and hydroxyproline (Hyp) amino acids to graphene (Gr), metal-doped graphene (MGr) and graphane (Gra) by means of quantum first-principles methods, in particular density functional theory (DFT) and *ab initio* molecular dynamics simulations (AIMD). DFT is a first-principles approach that has already been demonstrated to describe interactions in Gr–AA [27,28], H-metal-

E-mail address: c.silva@ucl.ac.uk.

0040-6090/$ – see front matter © 2010 Elsevier B.V. All rights reserved.
doi:10.1016/j.tsf.2010.06.068

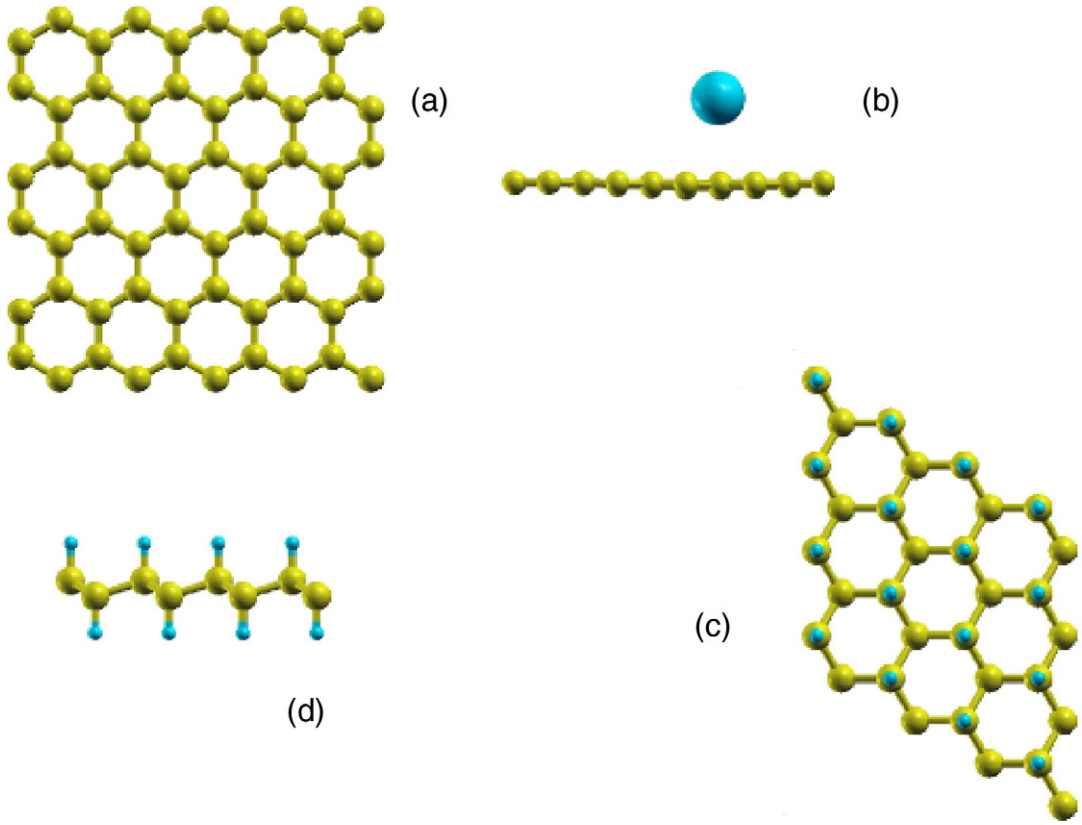

Fig. 1. Optimized geometries of Gr (a), Ca-doped Gr (b) and Gra (c and d). C atoms are colored in yellow, O in red, H in blue, N in grey and Ca in blue (big sphere).

organic frameworks [29] and benzene-metal complexes correctly [30], being in some cases as accurate as the more intricate method second-order M⊘ller–Plesset perturbation theory (MP2). Therefore, DFT already seems a fairly accurate computational approach for present purposes. Nevertheless, we have performed MP2 calculations on a small model system consisting of a hydrogen-passivated piece of graphene and Gly amino acid in order to assess the performance of the DFT method at describing Gr–AA composites. The results of this test presented in this work show that DFT predictions on Gr–AA systems can be considered as reasonably accurate.

The structure and stability of Gly (NH_2-CH_2-COOH), Pro (NH2-C_4H_7-COOH) and Hyp (NH_2-C_4H_6(OH)-COOH) amino acids have been studied intensively in the last decade by means of experiments and with theory because of their biological interest [31–33]; these are the unit blocks of long polypeptide chains that self-assemble in a multistep process to form collagen, the main building block of connective tissue in animals and the most abundant protein in mammals. Apart from its biological relevance, collagen also has been used widely as biomaterial in numerous medical applications, for instance, to enhance implant biocompatibility, as component of drug delivery systems and to create skin/bone tissue replacements (see Review by Lee *et al.* [34] and references in there).

There is previous theoretical work done on the binding of collagen AAs to carbon-based nanostructures and targeted surfaces. Recently, the adsorption of collagen AAs on hydroxyapatite surfaces (a mineral composite which is present in bones and is important for hard tissue replacement in dental and orthopedic applications) has been reviewed by several authors using techniques like DFT [35] and molecular dynamics performed with semi-empirical potentials [36]. Also recently Roman et al. [37] have investigated the adsorption of Gly on single-walled carbon nanotubes and graphene with DFT, although some of the simplifications assumed in their work deserve further examination (we will comment on this in the Results section of this article). The interactions of Gly with and Pro with oxide surfaces [38–41], silica [42,43], alumina [44,45] and metallic interfaces [46] have also been examined due to relevance to possible industrial applications and for providing improved understanding of bio-inorganic systems. Interestingly, the dynamics and adsorption of

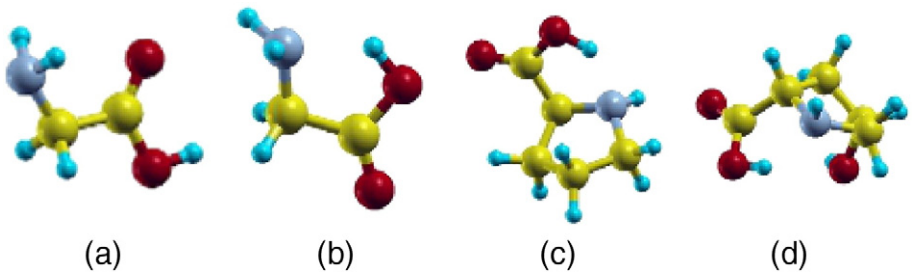

Fig. 2. Optimized geometries of Gly (a, b), conformers I-II respectively, Pro (b) and Hyp (c) amino acids. C atoms are colored in yellow, O in red, H in blue and N in grey.

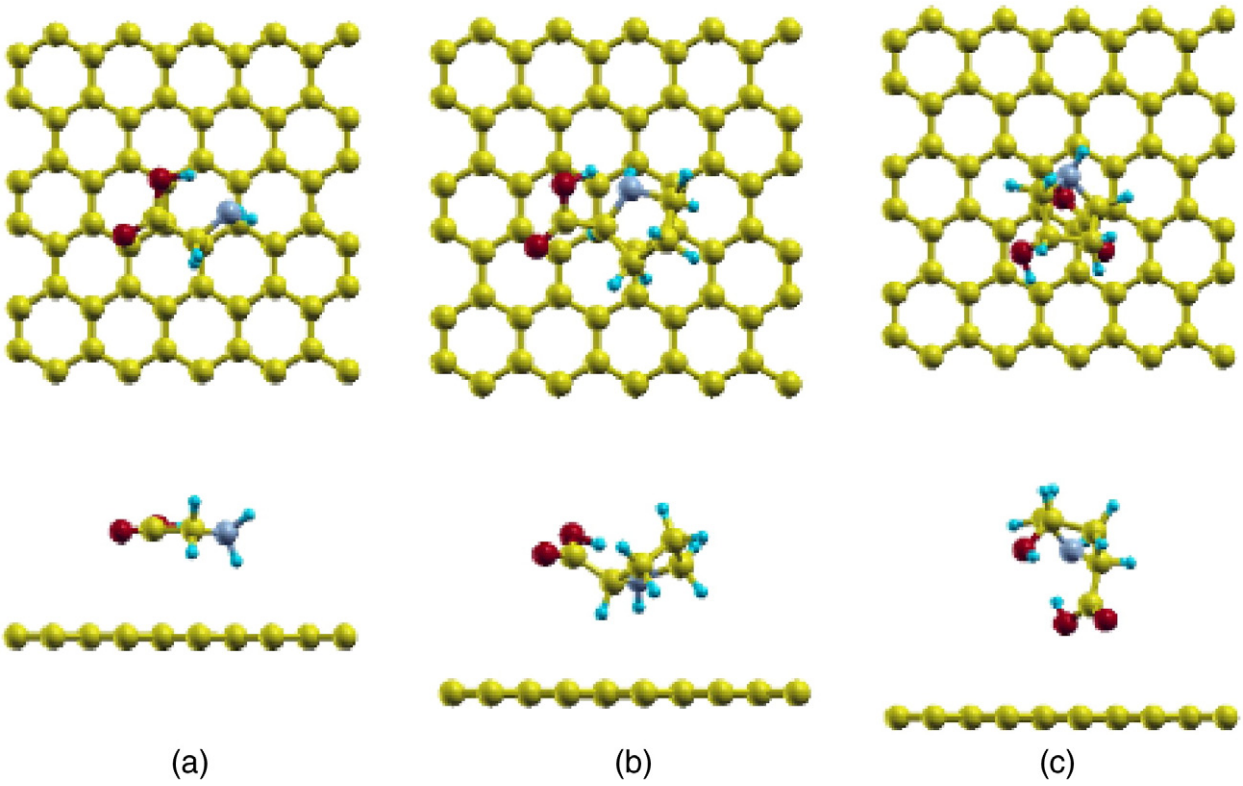

Fig. 3. Optimized geometries of Gly (a), Pro (b) and Hyp (c) adsorbed on Gr. Top and front views are shown for a good visualization of the systems.

collagen-like peptides on CNTs [47] and Ti-based material surfaces [48] immersed in water have been investigated using classical molecular dynamics simulations. In particular, authors of work [47] have demonstrated that collagen-like peptides may encapsulate spontaneously, although very slowly, into the inner space of CNTs due to an interplay between van der Waals and hydrophobic interactions. Despite of these investigations, there is lack of studies dealing with the quantum interactions of collagen-like peptides with CNSs and CSs (that is, considering possible charge transfers and electronic exchange interactions) basically due to the large computational cost and technical intricacies arising from the rich variety and large number of atomic bonds involved. However, this type of investigations is necessary to fully understand collagen-carbon nanohybrids and to address major unresolved issues as for instance possible toxicity of CNSs in physiological environment [22,49,50] wisely.

The main motivation of this work is to start filling this knowledge void. In particular, we focus here on two fundamental matters: (i) the interactions of collagen AAs with graphene at the quantum level of description, and (ii) how these interactions are affected by metal-doping and hydrogenation of graphene. The interest of studying the binding of collagen AAs to metal-doped Gr is that mediated π-metal-π interactions may result stronger than pure $\pi-\pi$ interactions, which in general are weak and prominent in bio-inorganic systems (for

Table 1
Adsorption energies of collagen AAs onto Gr and corresponding structural parameters.

AA	E_{ads}(eV)	d^{min}_{AA-Gr} (Å)	d^{AA}_{H-N} (Å)	d^{Gr}_{C-C} (Å)
Gly − I	−0.062	2.91	4.41	1.43
Gly − II	−0.098	2.78	1.85	1.43
Pro	−0.073	2.62	1.77	1.43
Hyp	−0.082	3.32	1.81	1.43

d^{min}_{AA-Gr} indicates the minimum distance between the AA and C atom in Gr, d^{AA}_{H-N} the distance between the H atom of the carboxyl end and N atom in the amine group of the AA, and d^{Gr}_{C-C} the distance between two neighboring C atoms in Gr.

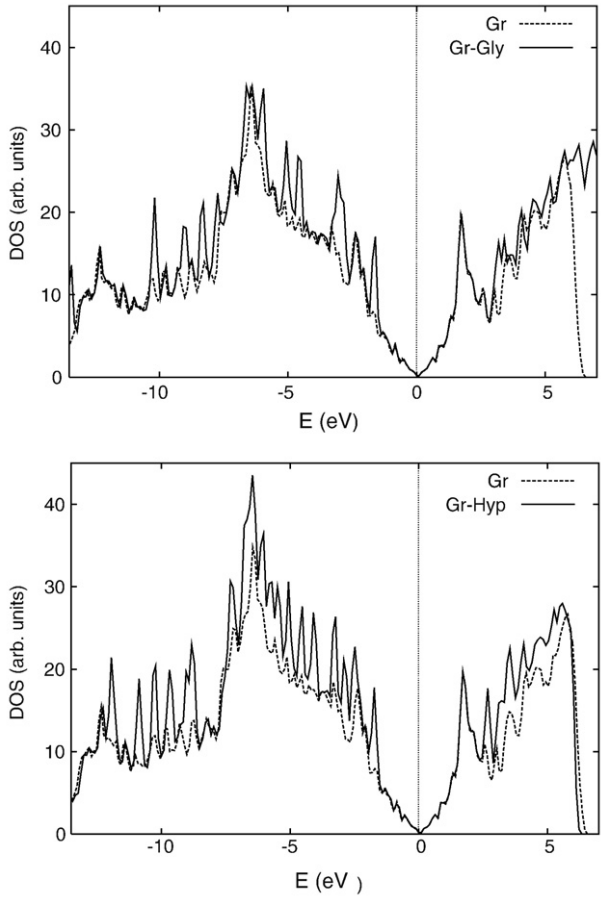

Fig. 4. DOS corresponding to geometry-optimized graphene and Gr–AA systems (AA = Gly, left; AA = Hyp, right). Fermi energy levels have been shifted to zero.

instance, $\pi-\pi$ interactions are relevant for understanding the adsorption of small nucleotides on the walls of CNTs [51,52]). In particular, we analyze calcium (Ca) doping because (i) Ca is already an abundant element in bones and muscles so in principle this seems to be a suitable doping for potential applications in biomedicine/biology, and (ii) due to their ability in losing electrons and the role of empty *d*-orbitals, Ca atoms have been already demonstrated to reinforce the binding of some aromatic AAs to CNTs and Gr [27]. In fact, we will show here that the effect of doping Gr with Ca atoms is to induce much stronger adsorption of Gly, Pro and Hyp amino acids on Gr. Concerning Gra, this is a fully saturated hydrocarbon derived from Gr wherein C atoms are bonded to H atoms alternating both sides of the plane and forming sp^3 hybridizations. Possible uses of graphane in biotechnological applications have not been investigated yet due to its very recent discovery and synthesis [5,6]. Gra may be of relevance in the design of biomaterials because it exhibits similar physical properties to those of Gr but with the possibility of tuning them by varying the concentration of H atoms; also biomolecules of interest could be immobilized on its surface via weak hydrogen-bond-mediated interactions. The results and conclusions reported in this work are valuable for advancing knowledge in modeling of biomaterials and to provide fundamental insights on the interactions of collagen components with CNSs/CSs.

2. Theoretical methods and computational details

DFT calculations have been performed within the projector augmented wave (PAW) scheme derived by Blöchl [53] and as implemented in the VASP code [54,55]. The exchange-correlation energy in the Kohn–Sham equations is approximated using the generalized gradient functional due to Perdew–Burke–Ernzerhof (GGA-PBE) [56]. Energy cut-offs have been set to 400 eV for carbon (C), oxygen (O) and nitrogen (N) atoms and to 250 eV for hydrogen (H). Regarding electronic states in valence, we consider s^2p^2 in C, s^2p^3 in N and s^2p^4 in O atoms.

Full atomic geometry relaxations have been carried out using a conjugate-gradient algorithm that keeps the volume of and shape of the unit cell fixed. In order to estimate the adsorption energy, E_{ads}, of Gly, Pro and Hyp amino acids to graphene, Ca-doped graphene and graphane we use the expression

$$E_{ads} = E_{system} - (E_{surf} + E_{AA}) \ , \tag{1}$$

where E_{system} is the total energy of the fully geometry optimized CS–AA system and the other two terms correspond to the energy of the CS and AA independently relaxed (in the Ca-doped Gr–AA case, E_{surf} represents the energy of the composite Gr-Ca atom system). According to this definition, and completely ignoring thermal effects, a negative value of E_{ads} means that adsorption of the AA on the CS considered is thermodynamically favorable. An atomic force tolerance of 0.05 eV/Å and special Monkhorst–Pack [57] **k**-point grid of $2\times2\times2$ have been imposed in all geometry optimizations; we have checked the adequacy of these parameters by monitoring the dependence of the total energy on them and imposing a convergence of less than 1 meV (the energy tolerance in the self-consistent cycles is 10^{-5} eV). In order to generate optimal initial CS–AA configurations, we first optimize all CS (see Fig. 1) and AA (see Fig. 2) structures separately and then place the resulting AA geometries at a distance of ~2 Å over the plane of the CSs considering different orientations. At least, 4 different AA orientations have been considered in each case, namely, (i) the carboxyl group of the AA (COOH) directed towards the CSs, (ii) the amine group of the AA (NH_2) directed towards the CSs and (iii and iv)

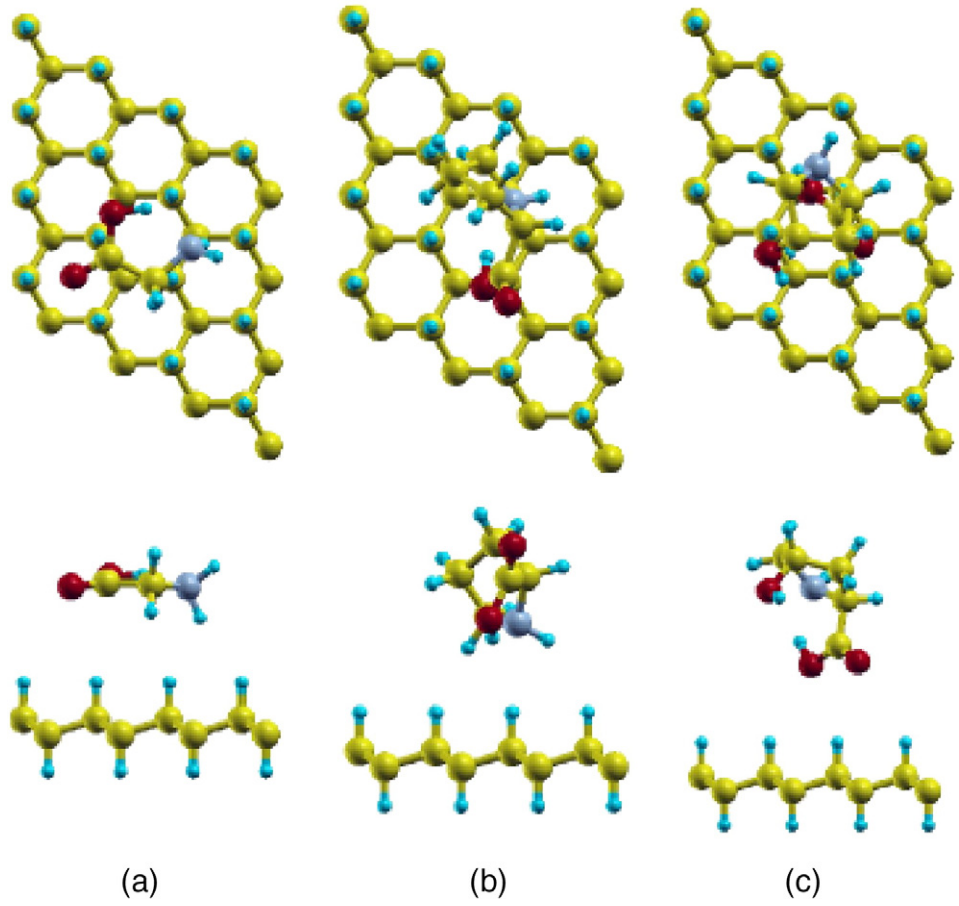

Fig. 5. Optimized geometries of Gly (a), Pro (b) and Hyp (c) adsorbed on Gra. Top and front views are shown for a good visualization of the systems.

the plane defined by the pentagonal AA ring parallel (inwards and outwards) to the carbon-surface plane.

Only neutral AA configurations have been analyzed in this study. Zwitterions, which are the preferred configurations of AAs in water, are observed to rearrange to their neutral form upon geometry optimization (as already has been reported by other authors [35,58]) so we leave the study of hydratation effects on CS–AA systems for future work. In our calculations, Gr is modeled with a 60 C atom plane and Gra with 32 C and 32 H atoms. The dimensions of the simulation box are typically $12.5\times13.0\times25.0$ Å where periodic boundary conditions are applied to all directions; the size of the simulation box has been chosen in order to avoid spurious AA–AA interactions between neighboring replica images.

As will be shown later, the calculated adsorption energies of Gly, Pro and Hyp on Gr and Gra are negative yet quite small in magnitude ($|E_{ads}|\sim20-90$ meV). In order to get insight into the effect of thermal excitations on the binding of collagen AAs to Gr and Gra, we have carried out a series of *ab initio* molecular dynamics simulations (AIMD) of composite CS–AA systems at ambient temperature ($T=300$ K). In AIMD simulations, a Verlet-type algorithm and Nosè thermostat are used for integration of Newton's equations of motion and sampling of the canonical ensembles, respectively. The size of the systems in the AIMD runs is the same than used in the atomic structural relaxations although given the intensive computational cost involved on these calculations, we employ Γ-point sampling only. The real time duration of a typical CS–AA molecular dynamics simulation is ~7 ps, being 10^{-3} ps the time step used. Initial configurations in the AIMD simulations correspond to the optimized geometries obtained in the structural atomic relaxations.

3. Results

3.1. CS and AA geometry optimizations

First, we have geometry optimized the Gr, Gra, Ca-doped Gr and AAs systems separately as explained in Section 2. For Gr, we obtain an interatomic C–C distance d_{C-C} of 1.42 Å , while for Gra, $d_{C-C}=1.53$ Å and $d_{C-H}=1.11$ Å (see Fig. 1). These figures are in excellent agreement with previous first-principles calculations and experimental data [4–6,59]. Concerning Ca-doped Gr, we have explored different possible adsorption sites of the impurity atoms on Gr (namely, customary *bridge*, *top* and *hole* positions) at concentration 1.67% (1 Ca atom per 60 C atoms) and found that the *hole* of the carbon hexagons is energetically the most favorable adsorption site. The adsorption energy corresponding to this preferred configuration is $E_{ads}=-0.391$ eV, being $d_{Ca-C}=2.19$ Å the distance between the Ca impurity and nearest C atom. The mechanism by which the calcium atom adsorbs on the carbon surface involves an electronic charge transfer of $-1.1e$ from the impurity (donor) to the surface. This result is obtained by performing charge-density distribution (CDD) analysis based on the Bader theory [60,61]; with this approach essentially one calculates the atomic charges by decomposing the total electronic charge density into atomic contributions that localize in regions bounded by minima of the charge density.

Regarding collagen AAs, we have considered two different Gly conformers (referred to as Gly-I and Gly-II), one Pro and one Hyp (see Fig. 2). It is well-known that a number of stable but structurally different AA configurations can be found in the gas phase [44,62] so we have assessed the effect of atomic AA structure on our final results for Gly. As it will be shown later, changes in the atomic structure of Gly do not affect appreciably our general statements so agreeably the same can be expected for Pro and Hyp. (If nothing is specified throughout, Gly refers to conformer II.)

Concerning the geometry relaxations, we find that our optimized AA structures are in very good agreement with respect to previous *ab initio* results obtained with a LCAO implementation of DFT [35]. In particular, we find that the distance between the H atom contained in the carboxyl AA group and N atom of the amine group is 1.86 Å in Gly-II, 1.79 Å in Pro and 1.82 Å in Hyp (see Fig. 2). Reproducibility of previously reported *ab initio* results and measurements provides confidence about the accuracy of the methodology employed throughout. However, in order to test the reliability of the DFT-PBE method at describing weak collagen AA–CS interactions we have performed additional calculations on a small model system using the MP2 approach. Results of this test are presented in Section 3.6.

Table 2
Adsorption energies of collagen AAs onto Gra and corresponding structural parameters.

AA	E_{ads}(eV)	d^{min}_{AA-Gra} (Å)	d^{AA}_{H-N} (Å)	d^{Gra}_{C-C} (Å)
Gly − I	−0.045	2.28	4.41	1.53
Gly − II	−0.081	2.33	1.84	1.53
Pro	−0.054	2.10	1.78	1.53
Hyp	−0.028	2.26	1.79	1.53

d^{min}_{AA-Gra} indicates the minimum distance between the AA and H atom in Gra, d^{AA}_{H-N} the distance between the H atom of the carboxyl end and N atom in the amine group of the AA, and d^{Gr}_{C-C} the distance between two neighboring C atoms in Gra.

3.2. AA adsorption on graphene

We report here the lowest-energy Gr–AA structures resulting from our full geometry optimizations in which different AA orientations relative to the carbon surface and adsorption sites have been considered. For Gly, we find that adsorption on Gr is thermodynamically favorable (that is, $E_{abs}<0$) in all the studied

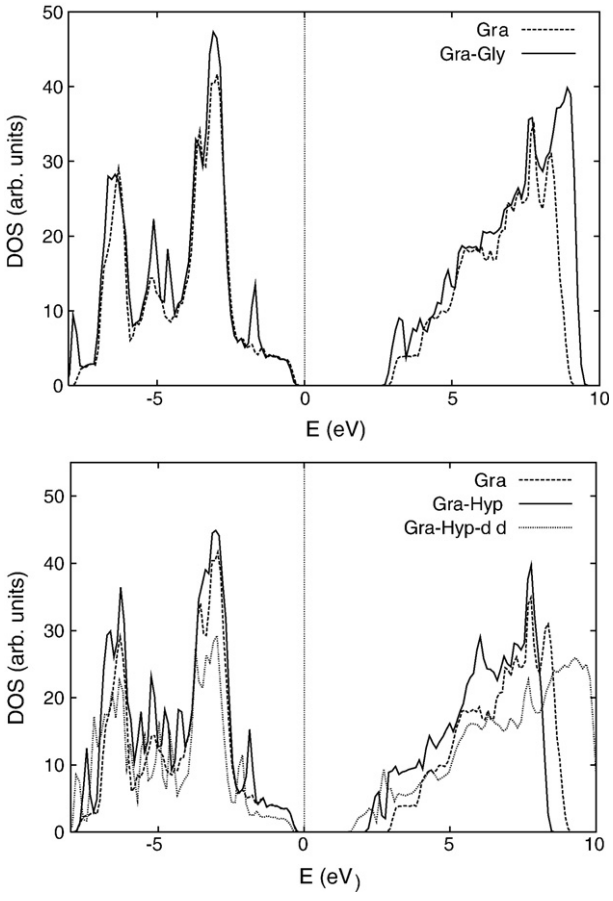

Fig. 6. DOS corresponding to geometry optimized graphane and Gra–AA systems (AA = Gly, left; AA = Hyp, right). Fermi energy levels have been shifted to zero.

cases (conformers I and II). In particular, the smallest E_{abs} value is obtained when the plane defined by atoms C–N–C in Gly-II is oriented parallel to the carbon surface (see Fig. 3(a) and Table 1). This configuration bears the signature of weak $\pi-\pi$ interactions, which are also present in Gr–aromatic AA complexes and CNT–DNA nucleobase hybrids [28,63]. In this most favorable case, E_{ads} amounts to −0.098 eV which indicates very weak binding of Gly to the graphite sheet. In Ref. [37], Roman et al. already investigated the binding of Gly to single-walled carbon nanotubes and graphene; in that work, the authors concluded that neutral Gly adsorbs onto Gr through the carboxyl end and that the corresponding E_{ads} value is −0.04 eV. According to our calculations, however, adsorption of Gly by the carboxyl group leads to an energy of $E_{ads}=-0.08$ eV, so that the already described configuration plotted in Fig. 3(a) is energetically more favorable than this by practically 20 meV. We believe that the reason for such disagreements is threefold, namely in Ref. [37] (i) full Gr–Gly geometry optimizations were not carried out (Gly was not geometry optimized but its structure remained fixed), (ii) only Gly orientations involving either the carboxyl or amine groups directed towards the plane of the carbon surface were considered, and (iii) a small Gr supercell (only 18 atoms) was used in the simulations so is likely that results include the effect of Gly–Gly interactions between neighboring images.

Regarding Pro, we also find positive and weak binding to graphene independently of the AA orientation considered. Estimated E_{ads} energies are somewhat larger than obtained in the Gr–Gly system (see Table 1). At difference with Gly, adsorption of Pro onto Gr is favored by placing the amine group of the amino acid closer to the carbon-surface and tilting the plane of its pentagonal ring slightly with respect to Gr (see Fig. 3(b)). In the Hyp case, strongest binding occurs when the carboxyl group is directed towards the carbon-surface and the amine group placed away (see Fig. 3(c)). Like in the Gly and Pro cases, the binding of Hyp to Gr is very weak.

In Table 1, interatomic distances on final optimized geometries are reported. In general, it is observed that Gr and AAs do not distort significantly with respect to their isolated optimized forms when joining to form Gr–AA systems.

An interesting application of carbon-based nanostructures is that of sensing of molecules [13,14,20]. The principle upon which these applications work is that changes on the electronic/optical properties of the nanostructure in question can be unequivocally identified with the entities that attach to its surface. The more dramatic the changes on the well-known physical properties of CSs/CNs, the more effective the sensing is. Motivated by such a possibility in what collagen AAs and graphene concerns, we have explored changes in the electronic structure of graphene when Gly and Hyp adsorb onto it. In particular, we have calculated the density of electronic states (DOS) of geometry optimized Gr (a zero-gap material with two linear bands crossing at the Dirac point [64]) and Gr–AA systems. In order to obtain accurate DOS plots, we have increased the k-point mesh used for first Brillouin zone (IBZ) sampling up to $8\times8\times2$. In Fig. 4, we show the results of these calculations. As can be observed, the shape of both Gr and Gr–AA DOSs is practically identical within the region around the Fermi energy level, E_F (shifted to zero in the figure), and no band gap is induced to open on the electronic structure of Gr. Since occupied electronic states with energy close to E_F are the ones responsible for the optical/electronic properties of a material, it can be concluded that Gr-based nanostructures are in principle not suitable for efficient sensing of collagen amino acids.

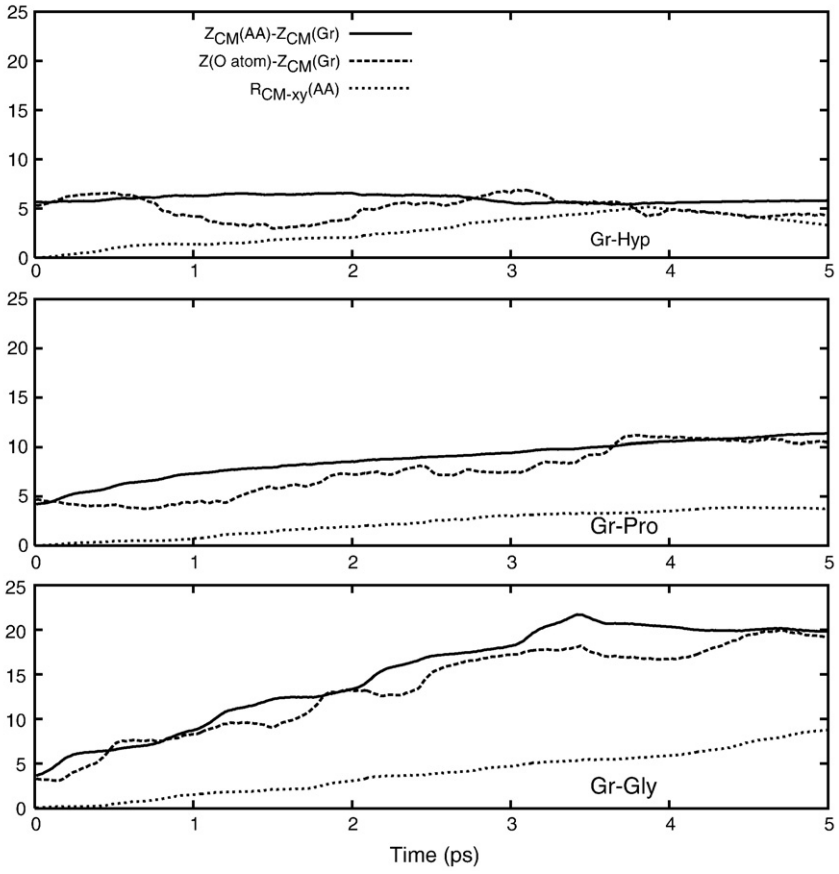

Fig. 7. Monitoring of the AA center of mass (CM) trajectories generated along AIMD simulations of joint Gr–AA systems performed at room temperature. Distances are in units of Å.

3.3. AA adsorption on graphane

As noted in the Introduction, one of the objectives of this study is to assess the effects of graphene hydrogenation on the quantum interactions of collagen AAs with Gr. Graphane is a material, first predicted by theoretical means and then realized in the laboratory [5,6], which bears some physical similarities with Gr, but also some differences. For instance, Gra is an insulator material with an electronic band gap width of $E_{gap}=3.1$ eV (according to our calculations). Therefore is engaging to start exploring possible applications of Gra in bio and nanotechnology fields.

Likewise to the previous Gr case, we have analyzed the adsorption of Gly, Pro and Hyp on top of Gra considering different AA orientations and adsorption sites. In Fig. 5, energetically most favorable Gra–AA geometries are shown. As can be observed, these configurations are quite similar to the Gr–AA ones depicted in Fig. 3 in what AA orientation concerns. In particular, Gly is oriented parallel to Gra while Pro and Hyp place their amine and carboxyl group, respectively, close to the CH-based surface. A look at Table 2 reveals that collagen AA binding to Gra is even weaker than that corresponding to Gr.

We have also investigated the possibility of using Gra for sensing of collagen AAs by performing accurate DOS analysis of the relaxed Gra and Gra–AA structures. Results of these calculations are shown in Fig. 6. It is observed that AA binding to Gra causes partial closure of its electronic band gap, being most noticeable in the Hyp case where the value of the band gap decreases down to $E_{gap}=2.2$ eV. In view of this effect, we have proceeded to increase the number of Hyp units onto Gra in order to discern whether such behavior scales or not with the number of AAs. It is found that E_{gap} decreases from 2.2 to 1.7 eV when the number of adsorbed Hyp amino acids is doubled (case shown in Fig. 6 as "dd"). This result comes to show that the width of the electronic band gap of Gra can be tuned by attaching different number and species of AAs onto it. Despite that we do not observe total closure of the band gap, it can be concluded that Gra appears to be a suitable material for engineering applications of collagen AAs sensing, especially of Hyp. The causes of this electronic band gap variation remain unclear to us although partial oxidization of Gra could be suggested on basis of what is observed in Gr [65] and the adsorption geometry of Hyp (carboxylate group pointing down to the hydrogenated carbon surface). We leave further investigations on such intriguing effect for future work given its possible relevance in nanoelectronics. Finally, the value of the d_{C-C}^{Gra} parameter reported in Table 2 shows that no particular deformation of Gra due to amino acid adsorption occurs.

3.4. Molecular dynamics simulations

In Sections 3.2 and 3.3, we have shown that Gly, Pro and Hyp bind very weakly to Gr and Gra, the corresponding adsorption energies being of order $\sim 10^{-2}-10^{-3}$ eV. Although joint Gr(a)-collagen AA systems should remain stable at low temperatures, room-temperature thermal excitations could be strong enough to induce AA-desadsorption from Gr and Gra since the value of the Boltzmann factor at $T=300$ K already amounts to $k_BT=0.026$ eV. With the aim of exploring this possibility, we have conducted a series of *ab initio* molecular dynamics (AIMD) simulations of Gly, Pro and Hyp onto Gr and Gra as explained in Section 2.

In Figs. 7 and 8 results of our AIMD simulations are presented, where details of the trajectory of the center of mass (CM) of the amino acid with respect to the all-effects translationally static carbon-based

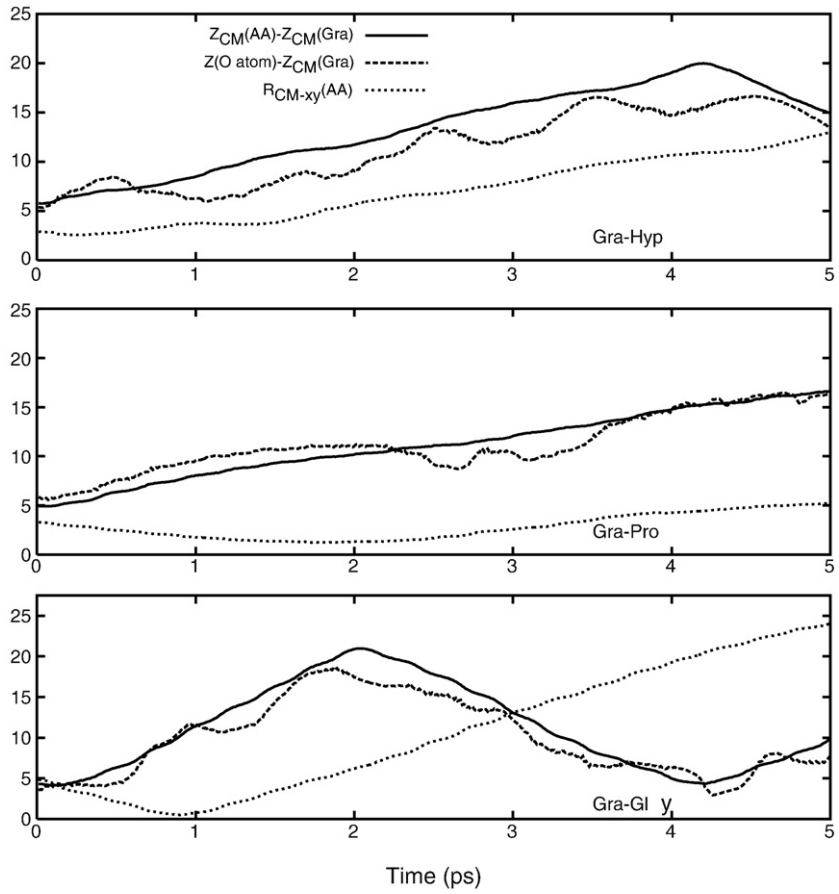

Fig. 8. Monitoring of the AA center of mass (CM) trajectories generated along AIMD simulations of joint Gra–AA systems performed at room temperature. Distances are in units of Å.

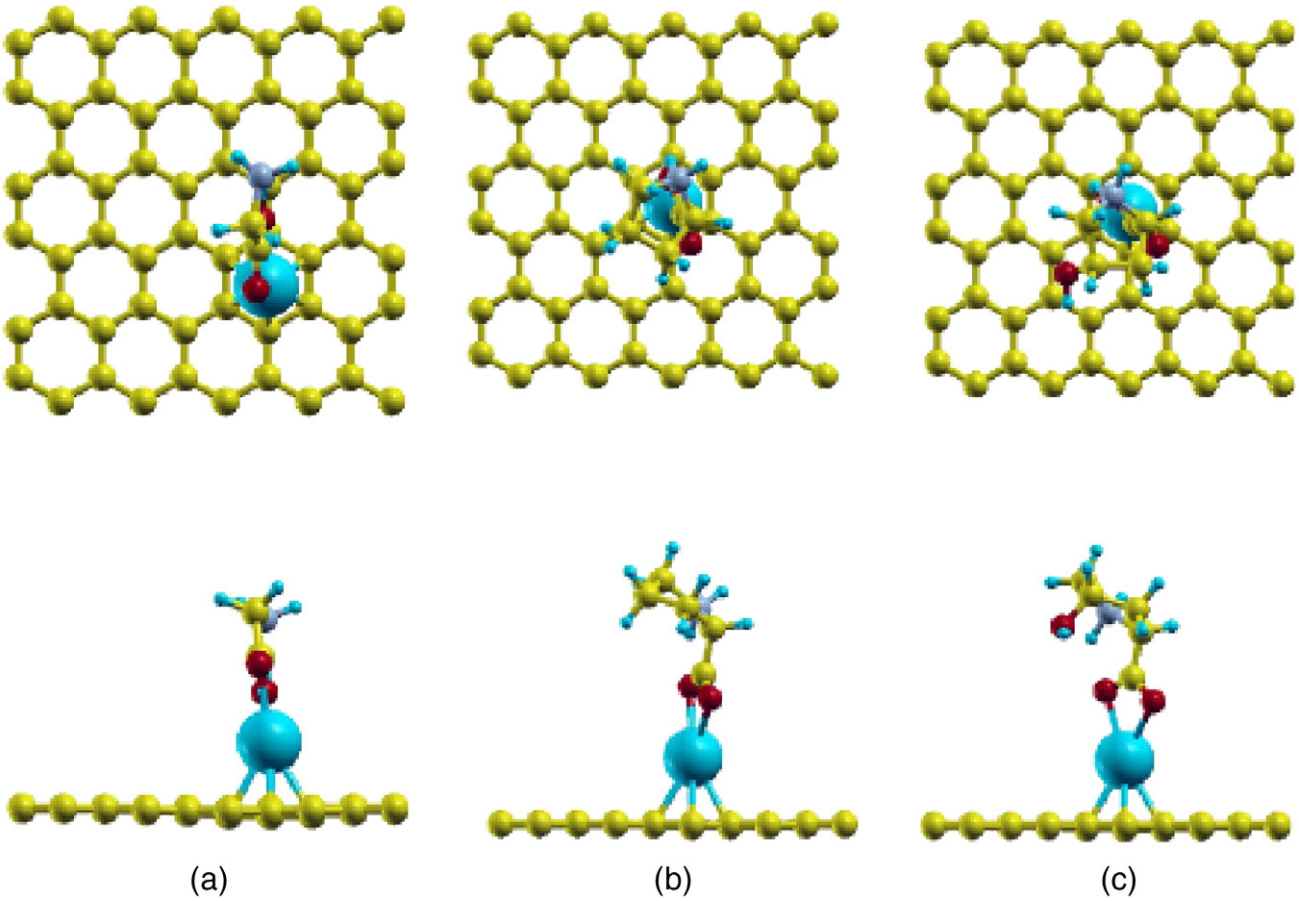

Fig. 9. Optimized geometries of Gly (a), Pro (b) and Hyp (c) adsorbed on Ca-doped Gr. Top and front views are shown for a good visualization of the systems.

surface are included. Specifically, we plot the *z*-component (out-of-plane) and *x-y* projection (in-plane) of the CM position of the amino acid, and position of the O atom in the AA carboxyl group. Account of the O atom trajectory is useful to determine whether the AA rotates or not since the difference between curves Z(O atom) − Z_{CM}(Gr) and Z_{CM}(AA) − Z_{CM}(Gr) in the figures provides this information directly (i.e., in case of free AA rotation Z(O atom) − Z_{CM}(AA) must fluctuate around zero-value otherwise remain constant). From the Gr–AA AIMD results shown in Fig. 7, several room-temperature-induced effects are observed: (i) Gly desadsorbs from Gr and diffuses through the volume of the container while rotating, (ii) Hyp does not deattach from the Gr surface though it moves slowly through the *x-y* plane and it rotates, and (iii) Pro exhibits an intermediate behavior between Gly and Hyp although its tendency clearly is to deadsorb from Gr. These conclusions have been cross-checked by visual inspection of MD animations recreated from the configurations generated in the AIMD runs.

Table 3
Adsorption energies of neutral collagen AAs onto Ca-doped Gr and corresponding structural parameters.

AA	E_{ads}(eV)	d^{min}_{AA-Ca} (Å)	d^{AA}_{H-N} (Å)	d^{Gr}_{C-C} (Å)
Gly − I	−1.166 (−1.733)	2.21 (2.08)	4.43 (4.57)	1.43 (1.43)
Gly − II	−1.488 (−2.342)	2.35 (2.29)	1.76 (4.33)	1.43 (1.43)
Pro	−2.067 (−2.298)	2.37 (2.30)	1.06 (4.64)	1.43 (1.43)
Hyp	−2.076 (−2.342)	2.38 (2.30)	1.06 (4.82)	1.43 (1.43)

Figures within parentheses correspond to anionic AA species adsorbed onto hydrogenated Ca-doped Gr. d^{min}_{AA-Ca} indicates the minimum distance between the AA and Ca atom, d^{AA}_{H-N} the distance between the H atom of the carboxyl end (or bonded to the Ca impurity) and N atom in the amine group of the AA, and d^{Gr}_{C-C} the distance between two neighboring C atoms in Gr.

Regarding Gra–AA systems, similar thermal-excitation effects than assessed in the similar Gr–AA systems are observed (see Fig. 8). Only small differences like larger diffusion of the AA center of mass in all the cases and Hyp desadsorption from Gra are noticed.

Summing up the AIMD results, it is found that joint Gr–AA and Gra–AA systems are in principle stable only at low temperatures, that is to mean, well below room temperature.

3.5. AA adsorption on Ca-doped graphene

In view of the weak binding of Gly, Pro and Hyp to Gr and Gra and corresponding temperature-induced AA desadsorption described in Sections 3.2, 3.3 and 3.4, it turns out to be appealing to explore ways of strengthening Gr–AA interactions in order to attain much more stable Gr–AA hybrids at room temperature. A likely avenue to attain this consists in chemically functionalizing Gr by doping it with a suitable element or compound. As noted in the Introduction, we have chosen to study here the effect of Ca impurities on Gr–AA interactions because Ca is a good charge donor which is already present in considerable proportion in connective and musculo-skeletal tissues [66,67]. Also Ca-doping has been proved to enhance $\pi-\pi$ interactions of Gr with dioxin monocyclic organic compound (C_4H_4O), which structurally is similar to collagen AAs [27].

In Fig. 9, we display the most favorable configurations deriving from our geometry optimization runs. Like in the Gr–AA case, different AA orientations have been considered with respect to the Gr surface although this time on top of the impurity atom. As is observed in the figure, most stable configurations now involve binding of the AA bodies to the Ca atom through the carboxyl end. Interestingly, estimated E_{ads} values decrease by practically two orders of magnitude with respect to non-doped Gr cases, being the Gr–Ca–Hyp binding the

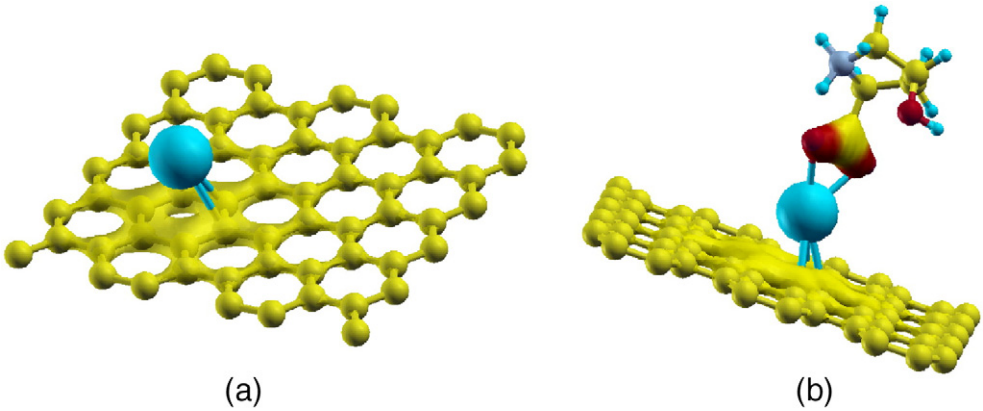

Fig. 10. Adsorption of the Ca impurity atom onto Gr (top). Adsorption of Hyp AA on Ca-doped Gr surface (bottom). In both plots, CDD analysis results are shown in which areas with accumulated electronic charge density are indicated with rough texture.

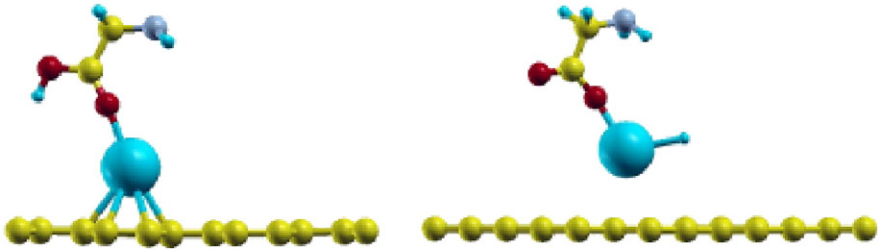

Fig. 11. Optimized conformation of neutral Gly-I adsorbed on Ca-doped Gr (left) and of anionic Gly-I adsorbed on hydrogenated Ca-doped Gr (right).

strongest (see Table 3). Such dramatic increase on the strength of the Gr–AA binding can be understood in terms of newly formed O–Ca bonds that result from electronic charge transfer between the impurity atom and the AA carboxyl group (sketched in Fig. 9 by solid rods). Interestingly, upon geometry optimization we observe proton transfer (H atom) from the carboxyl end to the amine group (which transform into COO^- and NH_3^+, respectively) in the Pro and Hyp cases (see value of parameter d^{AA}_{H-N} in Table 3) which correspond to the systems exhibiting smallest E_{ads} values. The cause for this proton transfer can be understood in terms of the argument already given, namely that formation of O–Ca bonds further stabilizes the Gr–AA systems, so destroying the carboxylic O–H bond in order to create an extra O–Ca one happens to be energetically favorable for Pro and Hyp. We have performed charge-density distribution (CDD) analysis [60,61] of the joint Gr–Ca–Hyp system in order to assess electronic charge redistributions within it. As could be foreseen, the CDD analysis shows that some electronic charge ($\sim -0.5e$) is transferred from the Ca impurity to the carboxyl group of the amino acid thus reinforcing the Gr–AA binding. At the same time, the charge redistribution within the AA leads to an electronic charge increase of $-0.2e$ in the N atom. The unravelled Ca–AA electronic charge transfer is sketched in Fig. 10 by denoting areas of accumulated electronic density with rough texture. Parameter d^{Gr}_{C-C} enclosed in Table 3 shows that structural distortions in Gr originated by adsorption of the Ca atom and AA on it are practically insignificant.

We have further analyzed the stability of Gr–Ca–AA complexes by considering possible Ca–AA segregation from the Gr surface. For this, we have geometry optimized joint Ca–AA units and proceeded to calculate the energy difference $E_{segr} = E_{Gr-Ca-AA} - E_{Ca-AA} - E_{Gr}$. In all the cases we find negative E_{segr} values (for instance, in the Hyp case E_{segr} amounts to -1.41 eV) so the studied hybrids are very unlikely to separate spontaneously into Ca-Hyp and Gr units. Moreover, the possibility of proton transfer from the carboxylic AA group to the Ca–Gr surface and subsequent adsorption of the resulting anionic species on the hydrogenated surface, has been also investigated. In all the studied cases, we find that this conformation further stabilizes the Gr–Ca–AA complexes. In particular, the largest E_{ads} reduction upon proton transfer is experienced by Gly (conformer II) and it amounts to -0.854 eV (see Table 3 and Fig. 11). This last result might suggest that Gr–Ca–AA systems could be further stabilized on basic water, or even more chiefly, that aggregation of AA units on Gr–Ca surfaces could be monitored/controlled via the basicity (that is, concentration of OH^- hydroxide ions) of the solvent if dissociation of water molecules on the Ca-centers occurred to be energetically favorable. These remarks, however, are rather speculative and further computational work is required for assessing them; it is noted that we are addressing work on this direction at the moment.

The main finding presented in this section, namely dramatic enhancement of Gr–collagen AA interactions by chemical functionalization of Gr with Ca atoms, suggests that inorganic nanostructures composed of Ca and Gr could be employed as surfaces for adhesion of

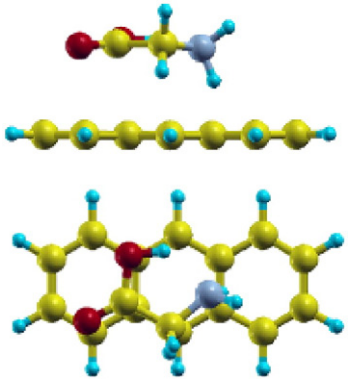

Fig. 12. System model composed of a hydrogen-passivated piece of graphene and Gly amino acid where MP2 and DFT-PBE calculations have been performed. The plot shows the final structure obtained in the DFT-PBE geometry optimization.

collagen polypeptides. This theoretical prediction can be useful for tailoring of nanostructures with potential application in biotechnology and biomedicine, particularly in the creation of artificial biomimetic surfaces able to adsorb on medical implants and designed to enhance biocompatibility properties.

3.6. MP2 versus DFT-PBE

In general DFT methods tend to underestimate binding energies in molecular systems. The reason of this shortcoming radicates on the inability to describe long-range forces of dispersive type, as for instance van der Waals (vdW), accurately. Nevertheless, numerous recent studies have proved the DFT-PBE method successful at evaluating $\pi-\pi$ interactions in comparison with more intricate, but also largely more expensive, computational approaches [27–30]. In order to check the reliability of the results presented in previous sections, we have performed calculations on a model system consisting of a small piece of graphene passivated by hydrogen atoms and a Gly amino acid (see Fig. 12) using the MP2 approach. In MP2 calculations electronic correlation effects are estimated accurately by means of the Rayleigh–Schrödinger perturbation theory and considering the Hartree–Fock Hamiltonian as the unperturbed system. MP2 calculations were performed with the GAUSSIAN03 package [68] using 6-31G++ basis sets including double diffuse functions. For comparison, DFT-PBE calculations were carried out on the same model system with identical technical parameters than reported in Section 2. Structural optimizations were performed with both approaches imposing a force tolerance of 0.02 eV/Å on the atoms. The conclusions deriving from these calculations can be summarized as: (i) both MP2 and DFT-PBE geometry optimized structures are practically identical (see Fig. 12) the only difference being that the distance between the Gly amino acid and the Gr rod is 3.60 Å in the MP2 case and 3.80 Å in the DFT-PBE case; and (ii) MP2 and DFT-PBE binding energies amount to −0.38 and −0.10 eV, respectively. On the light of these results, it can be concluded that the description of Gr–AA systems obtained with DFT-PBE is fairly accurate although the inclusion of subtle long-range interactions is likely to increase the binding of AAs to carbon-based surfaces.

4. Conclusions

In this *ab initio* computer simulation study, we have investigated the adsorption of glycine, proline and hydroxyproline amino acids, the major constituents of type I collagen protein, to graphene, graphane and Ca-doped graphene. In the Gr–AA and Gra–AA systems, room-temperature effects have been explored by carrying out a series of *ab initio* molecular dynamics simulations. Our study shows that the binding of collagen amino acids to Gr and Gra is thermodynamically favorable although very weak, so room-temperature effects can provoke AA detachment in most of the cases. Nevertheless, we find that by doping Gr with Ca atoms Gr–AA interactions are enhanced dramatically so corresponding adsorption energies decrease by practically two orders of magnitude ($-2.3<E_{ads}<-1.4$ eV). We have also analyzed the performance of Gr and Gra in possible sensing application of collagen AAs; we predict that, while Gr is hardly sensitive, Gra undergoes noticeable changes in electronic structure as result of Hyp adsorption.

In this work, we provide fundamental knowledge on quantum Gr–collagen AA interactions, scarcely investigated so far, which can be exploited in fields like biomaterials modeling and probably also nanoelectronics. In future work, we will analyze the interactions of collagen-like peptides with carbon-based surfaces using computational approaches less intensive than employed here, as for instance hybrid QM/MM (Quantum Mechanical/Molecular Mechanics) techniques and the density-functional tight-binding method [69,70]. The results presented in this work will be used to evaluate the performance of available force fields that subsequently will be used in the planned QM/MM simulations. Given the biotechnological interest of these studies, the effect of water on CS-collagen interactions will be included. Work on this direction is already in progress.

Acknowledgments

The author is grateful to Dr. Denis Courtier-Murias for insightful discussions and acknowledges computational resources on the U.K. National Supercomputing HECToR service.

References

[1] S. Iijima, Nature (London) 354 (1991) 56.
[2] M.S. Dresselhaus, G. Dresselhaus, P.C. Eklund, Science of Fullerenes and Carbon Nanotubes, Academic Press, New York, 1996.
[3] M.L. Cohen, Science 261 (1993) 307.
[4] K.S. Novoselov, A.K. Geim, S.V. Morozov, D. Jiang, M.I. Katsnelson, I.V. Grigorieva, S.V. Dubonos, A.A. Firsov, Nature (London) 438 (2005) 197.
[5] J.O. Sofo, A.S. Chaudhari, G.D. Barber, Phys. Rev. B 75 (2007) 153401.
[6] D.C. Elias, R.R. Nair, T.M.G. Mohiuddin, S.V. Morozov, P. Blake, M.P. Halsall, A.C. Ferrari, D.W. Boukhvalov, M.I. Katsnelson, A.K. Geim, K.S. Novoselov, Science 323 (2009) 610.
[7] H.C. Schniepp, J.-L. Li, M.J. McAllister, H. Sai, M. Herrera-Alonso, D.H. Adamson, R.K. Prudhomme, R. Car, D.A. Saville, I.A. Aksay, J. Phys. Chem. B 110 (2006) 8535.
[8] S. Stankovich, D.A. Dikin, R.D. Piner, K.A. Kohlhaas, A. Kleinhammes, Y. Jia, Y. Wu, S.T. Nguyen, R.S. Ruoff, Carbon 45 (2007) 1558.
[9] C. Gomez-Navarro, R.T. Weitz, A.M. Bittner, M. Scolari, A. Mews, M. Burghard, K. Kern, Nano Lett. 7 (2007) 3499.
[10] A.K. Geim, K.S. Novoselov, Nat. Mater. 6 (2007) 183.
[11] Y. Zhang, Y.-W. Tan, H.L. Storner, P. Kim, Nature (London) 438 (2005) 201.
[12] D.A. Abanin, P.A. Lee, L.S. Levitov, Phys. Rev. Lett. 96 (2006) 176803.
[13] J. Kong, N.R. Franklin, C. Zhou, M.G. Chapline, S. Peng, K. Cho, H. Dai, Science 287 (2000) 622.
[14] S. Peng, K. Cho, Nano Lett. 3 (2003) 513.
[15] R.H. Baughman, C. Cui, A.A. Zakhidov, Z. Iqbal, J.N. Barisci, G.M. Spinks, G.G. Wallace, A. Mazzoldi, D. De Rossi, A.G. Rinzler, O. Jaschinski, S. Roth, M. Kertesz, Science 284 (1999) 1340.
[16] S. Tans, A. Verschueren, C. Dekker, Nature 393 (1998) 49.
[17] A.C. Dillon, K.M. Jones, T.A. Bekkedahl, C.H. Kiang, D.S. Bethune, M.J. Heben, Nature 386 (1997) 377.
[18] S.A. Shevlin, Z.X. Guo, J. Phys. Chem. C 112 (2008) 17456.
[19] R. Singh, D. Pantarotto, D. McCarthy, O. Chaloin, J. Hoebeke, C.D. Partidos, K. Kostarelos, J. Am. Chem. Soc. 127 (2005) 4388.
[20] S. Meng, P. Maragakis, C. Papaloukas, E. Kaxiras, Nano Lett. 7 (2007) 45.
[21] X. Chen, A. Kis, A. Zettl, C.R. Bertozzi, Proc. Natl Acad. Sci. 104 (2007) 8218.
[22] W. Yang, P. Thordarson, J.J. Gooding, S.P. Ringer, F. Braet, Nanotechnology 18 (2007) 412001.
[23] N. Park, S. Hong, G. Kim, S.-H. Jhi, J. Am. Chem. Soc. 129 (2007) 8999.
[24] R. Sorkin, A. Greenbaum, M. David-Pur, S. Anava, A. Ayali, E. Ben-Jacob, Y. Hanein, Nanotechnology 20 (2009) 015101.
[25] E. Ben-Jacob, Y. Hanein, J. Mater. Chem. 18 (2008) 5181.
[26] B.S. Harrison, A. Atala, Biomaterials 28 (2007) 344.
[27] H.S. Kang, J. Am. Chem. Soc. 127 (2005) 9839.
[28] C. Rajesh, C. Majumder, H. Mizuseki, Y. Kawazoe, J. Chem. Phys. 130 (2009) 124911.
[29] Y.Y. Sun, K. Lee, Y-H. Kim and S. B. Zhang, Appl. Phys. Lett. 95 (2009) 033109.
[30] H.S. Kang, J. Phys. Chem. A 109 (2005) 478.
[31] C.L. Jenkins, R.T. Raines, Nat. Prod. Rep. 19 (2002) 49.
[32] A. Lessarri, E.J. Cocinero, J.C. Lopez, J.L. Alonso, J. Am. Chem. Soc. 127 (2005) 2572.
[33] A.E. Aliev, D. Courtier-Murias, J. Phys. Chem. B 111 (2007) 14034.
[34] C.H. Lee, A. Singla, Y. Lee, Int. J. Pharmacol. 221 (2001) 1.
[35] N. Almora-Barrios, K.F. Austen, N.H. de Leeuw, Langmuir 25 (2009) 5018.
[36] H. Pan, J. Tao, X. Xu, R. Tang, Langmuir 23 (2007) 8972.
[37] T. Roman, W.A. Dinyo, H. Nakanishi, H. Kasai, Thin Solid Films 509 (2006) 218.
[38] S. Irrera, D. Costa, P. Marcus, J. Mol. Struc.:THEOCHEM 903 (2009) 49.
[39] E. Soria, E. Roman, E.M. Williams, J.L. de Segovia, Surf. Sci. 543 (1999) 433.
[40] T. Qiu, M.A. Barteau, J. Colloid Interface Sci. 303 (2006) 229.
[41] J. Lausmaa, P. Lofgren, B. Kasemo, J. Biomed. Mater. Res. 44 (1999) 227.
[42] M. Meng, L. Stievano, J.-F. Lambert, Langmuir 20 (2004) 914.
[43] C. Lomenech, G. Bery, D. Costa, L. Stievano, J.-F. Lambert, Chem. Phys. Chem. 6 (2005) 1061.
[44] C. Arrouvel, B. Diawara, D. Costa, P. Marcus, J. Phys. Chem. C 111 (2007) 18164.
[45] G. Tzvetkov, G. Koller, Y. Zubavichus, O. Fuchs, M.B. Casu, C. Heske, E. Umbach, M. Grunze, M.G. Ramsey, F.P. Netzer, Langmuir 20 (2004) 10551.
[46] G. Hong, H. Heinz, R.R. Naik, B.L. Farmer, R. Pachter, ACS Appl. Mater. Interfaces 1 (2009) 388.
[47] Y. Kang, Q. Wang, Y-C. Liu, T. Wu, Q. Chen and W-J. Guan, J. Phys. Chem. B 112 (2008) 4801.
[48] S. Monti, J. Phys. Chem. C 111 (2007) 6086.
[49] R. Chang, A. Violi, J. Phys. Chem. B 110 (2006) 5073.
[50] J. Liu, A.J. Hopfinger, Chem. Res. Toxicol. 21 (2008) 459.

[51] H. Gao, Y. Kong, D. Cui, Nano Lett. 3 (2003) 471.
[52] H. Gao, Y. Kong, Annu. Rev. Mater. Res. 34 (2005) 123.
[53] P.E. Blöchl, Phys. Rev. B 50 (1994) 17953.
[54] G. Kresse, D. Joubert, Phys. Rev. B 59 (1999) 1758.
[55] G. Kresse, J. Furthmüller, Phys. Rev. B 54 (1996) 11169.
[56] J.P. Perdew, K. Burke, M. Ernzerhof, Phys. Rev. Lett. 77 (1996) 3865.
[57] H.J. Monkhorst, J.D. Pack, Phys. Rev. B 13 (1976) 5188.
[58] Y.B. Ding, K. Kroghjespersen, Chem. Phys. Lett. 199 (1992) 261.
[59] D.W. Boukhvalov, M.I. Katsnelson, A.I. Lichtenstein, Phys. Rev. B 77 (2008) 035427.
[60] R.F.W. Bader, *Atoms in Molecules. A Quantum Theory*, Oxford University Press, New York, 1990.
[61] G. Henkelman, A. Arnaldsson, H. Johnsson, Comput. Mater. Sci. 36 (2006) 354.
[62] S.G. Stepanian, I.D. Reva, E.D. Radchenko, M.T.S. Rosado, M.L.T.S. Duarte, R. Fausto, L. Adamowicz, J. Phys. Chem. A 102 (1998) 1041.
[63] S. Gowtham, R.H. Scheicher, R. Ahuja, R. Pandey, S.P. Karna, Phys. Rev. B 76 (2007) 033401.
[64] A.H. Castro Neto, F. Guinea, N.M. Peres, K.S. Novoselov, A.K. Geim, Rev. Mod. Phys. 81 (2009) 109.
[65] J.-A. Yan, L. Xian, M.Y. Chou, Phys. Rev. Lett. 103 (2009) 086802.
[66] E. Bozler, Am. J. Physiol. 205 (1963) 686.
[67] P.L. Becker, J.J. Singer, J.V. Walsh Jr., F.S. Fay, Science 244 (1989) 211.
[68] GAUSSIAN03, M.J. Frisch, G.W. Trucks, H.B. Schlegel, G.E. Scuseria, M.A. Robb, J.R. Cheeseman, J.A. Montgomery Jr., T. Vreven, K.N. Kudin, J.C. Burant, J.M. Millam, S.S. Iyengar, J. Tomasi, V. Barone, B. Mennucci, M. Cossi, G. Scalmani, N. Rega, G.A. Petersson, H. Nakatsuji, M. Hada, M. Ehara, K. Toyota, R. Fukuda, J. Hasegawa, M. Ishida, T. Nakajima, Y. Honda, O. Kitao, H. Nakai, M. Klene, X. Li, J.E. Knox, H.P. Hratchian, J.B. Cross, V. Bakken, C. Adamo, J. Jaramillo, R. Gomperts, R.E. Stratmann, O. Yazyev, A.J. Austin, R. Cammi, C. Pomelli, J.W. Ochterski, P.Y. Ayala, K. Morokuma, G.A. Voth, P. Salvador, J.J. Dannenberg, V.G. Zakrzewski, S. Dapprich, A.D. Daniels, M.C. Strain, O. Farkas, D.K. Malick, A.D. Rabuck, K. Raghavachari, J.B. Foresman, J.V. Ortiz, Q. Cui, A.G. Baboul, S. Clifford, J. Cioslowski, B.B. Stefanov, G. Liu, A. Liashenko, P. Piskorz, I. Komaromi, R.L. Martin, D.J. Fox, T. Keith, M.A. Al-Laham, C.Y. Peng, A. Nanayakkara, M. Challacombe, P.M.W. Gill, B. Johnson, W. Chen, M.W. Wong, C. Gonzalez, J.A. Pople, Gaussian, Inc, Wallingford, CT, 2004.
[69] D. Porezag, Th. Frauenheim, Th. Köhler, G. Seifert, R. Kaschner, Phys. Rev. B 51 (1995) 12947.
[70] M. Elstner, D. Porezag, G. Jungnickel, J. Elsner, M. Hangk, Th. Frauenheim, S. Suhai, G. Seifert, Phys. Rev. B 58 (1998) 7260.